Design of an Implantable Antenna Feasibility Study for Continuous Glucose Monitoring

Pichitpong Soontornpipit[1], Member

ABSTRACT

The objective of this research was to design a patch antenna for communication with medical implants in the 402-405 MHz Medical Implant Communications Services band (MICS). Imbedded antennas used for biomedical telemetry such as cardiac pacemakers have been previously demonstrated for use either as sensing elements or as components of a wireless communication system. Designing an implanted antenna as a sensor is rather less difficult since the resonant frequency is seen to shift by changes in dielectric properties of the surrounding implanted areas affected by glucose levels. Based on our previous work of tissue characterization, an analytical technique can be developed to negate this frequency shift due to the change of permittivity and conductivity, from which the glucose levels are determined. This paper presents an antenna design used for communication from the implant to an external receiver, regardless of human tissue characterization. Using the genetic algorithm (GA) and the finite difference time domain (FDTD) method, the antenna is designed to have minimal detuning due to changes in blood glucose level. In this study, single and stacked nonhomogenous body layer for better performance were determined.

Keywords: Implantable Medical Devices, Implantable Antennas, Planar Inverted-F Antenna (PIFA), Waffle-Type Antenna.

1. INTRODUCTION

It is estimated that 23.6 million people (8% of population) in the United States, 48 million people (7.8% of population) in Europe, and 125 million people (9.2% of population) in Asia have diabetes, according to the Center for Disease Control and Prevention [1] as of 2011. In 2010, 700,564 people died due to the complications related to diabetes and 77,935 died from heart attacks [2]. Many of those patients even had cardiac pacemakers activated with implanted antennas inside. One of the reasons for this could possibly be the effect of glucose levels on the cardiac pacemaker that made implanted antennas malfunction [3]. Mostly, a diabetes condition affects insulin resistance in which there is an inability to control glucose levels in the blood stream. The change of glucose concentration from normoglycemia to hypoglycemia or hyperglycemia shifts the resonant frequency and thus lowers the characteristic performances of an implanted antenna. This is based on the fact that the glucose levels affect the dielectric properties of blood, muscle, fat and skin in which the antenna and biomedical devices are located [4]. These patients required frequent monitoring to avoid the effect of hyperglycemia or hypoglycemia. However, fasting blood glucose tests and other at-home monitoring procedures are painful methods [5]. Therefore, there has been a need for reliable and continuous monitoring technology for implantable cardioverter pacemakers and defibrillators to help patients better manage their medical treatments and avoid heart failures [6]. In order to reduce or totally eliminate the diabetes related deaths of cardioverter patients, a new generation of a pacemaker with a microwave antenna that has less sensitivity to the surrounding biological tissue is needed.

A biosensor system combining RF technologies is the key to developing the next generation of hyperthermia for medical treatments and monitoring various physiological parameters to improve the quality of a patient's life. In addition to medical therapy and diagnosis, biosensor technologies are regarded as important functions for implantable medical devices (heart and brain pacemakers, defibrillators, artificial eyes, cochlear implants, etc.), which need to transmit diagnostic information. In contrast to a number of research accomplishments related to hyperthermia, studies on implantable biosensors used to build the communication links between implanted devices and exterior instruments for biotelemetry are widely reported. These sensors can be implanted inside a human body along with the medical devices [7]. Regarding the Food and Drug Administration (FDA) and Federal Communication Commission (FCC), safety issues related to implanted devices in terms of maximum available powers at the receiver locations must be obtained. Furthermore, to provide the reliability of the communication link and estimate the minimum sensitivity requirement for the receiver, the radiation characteristics and 1-g averaged specific absorption rate (SAR) distributions are limited by American National Standards Institute (ANSI)/IEEE limitations [8]. These limitations protect the surrounding human tissues from being damaged from exposure to radiation.

Manuscript received on January 14, 2013 ; revised on March 27, 2014.

*The author is with Faculty of Public Health, Mahidol University, Thailand, E-mail: soontornpipit@gmail.com[1]

Considerable progress has been made in recent years to develop implantable sensors that can continually monitor or communicate with equipment inside or outside of the patient's body [9-14]. These advanced technologies in medical telemetry allow physicians to monitor patients' physiological parameters and communicate with internal medical devices using radio frequencies in order to modify functions/parameters on implanted biomedical devices. These devices require an integrated antenna in which the types of antennas depend on the implanted location. For instance, waveguide or low-profile antennas are externally positioned, and monopole or dipole antennas transformed from a coaxial cable are designed for internal use. Nevertheless, several types of antennas have been used or proposed for a variety of embedded wireless communication applications. Inductive antennas (coils of wire around a dielectric or ferrite core) have been successfully used for biomedical telemetry [14], although data rates are low, and size/weight and biocompatibility issues plague the coil-wound devices. To facilitate improvements in the communication range, the European Telecommunications Standards Institute (ETSI) reserved the MICS band for medical and meteorological applications. The MICS band occupies the spectrum from 402 to 405 MHz with a maximum emission bandwidth of 300 kHz [15]. Wire-type, microstrip, and planar invert-F antenna (PIFA) embedded in the human body were designed and analyzed for artificial eyes, cochlear implants, brain and cardiac telemetry. Designing antennas that would operate inside the human body is a challenging task. Factors such as human tissue dielectric property and conductivity, impedance matching, antenna size, specific absorb rate (SAR) requirements, and biocompatibility play an important role in the design.

In this study, our goal is to design an implanted antenna operating at 402-405 MHz MICS band. This small size antenna is mainly intended for use as a cardiac pacemaker and also for continuous glucose-monitoring applications. Fig. 1 shows the road map of the research activities reported in this paper. The antenna is a serpentine-shape PIFA with a superstrate cover to prevent the human tissues from shorting out the antenna and is shown in Fig. 2. Methods to reduce the size of the antenna by adding ground pins and using a high dielectric substrate material were applied. The antenna was simulated in a realistic human shoulder because pacemakers and implantable cardioverter defibrillators are normally placed between fat and muscle in the upper human chest. Simplified four-layer geometry (skin, fat, blood and muscle) from the human shoulder was used in a design process since the dimension of this simplified geometry could speed up the simulation time almost 50 percent [10]. Both uniform and non-uniform four-layer models are evaluated.

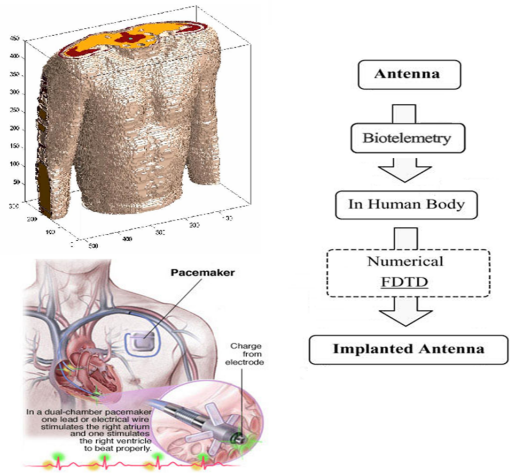

Fig.1: *Schematic Diagram of Research Activities.*

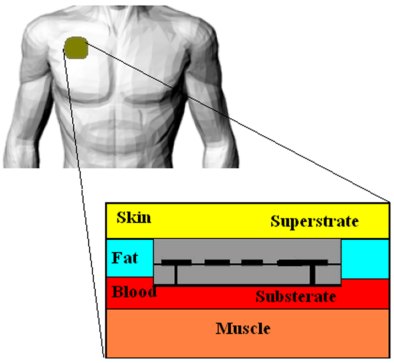

Fig.2: *Structure of an Implantable Antenna.*

The antennas are designed to operate in the 402-405 MHz band regardless of the changes in human tissues by different glucose levels by the genetic algorithm (GA) combined with a finite-difference time-domain (FDTD) solver. To measure the return loss of manufactured antennas, these antennas were tested in a three-layer fluid called TX-151 [16], the electrical characteristics of which were similar to those of the biological tissues on an HP8510C network analyzer.

This paper is organized as follows. Section II outlines the effect of glucose level on the dielectric properties of the human body. In Section III, we examine a design example to serve as the communication system and glucose sensor. In Section IV, the test results from a prototype antenna are compared with the simulation results.

2. EFFECT OF GLUCOSE ON THE DIELECTRIC PROPERTIES OF HUMAN BODY

This section discusses changes in the relative permittivity (ε_r) and the conductivity (σ) of human tissues (skin, fat, blood, and muscle) with glucose levels. In order to investigate the effect of glucose levels on

Table 1: *Dielectric Constant and Conductivities for Biological Tissues of the Simulation for Normoglycemia at 403 MHz [18 and 19]*

Tissue	ε_e	σ_e(S/m)
Fat	5.6	0.041
Skin	46.68	0.64
Skin(dry)	46.7	0.69
Skin(wet)	49.8	0.67
Muscle	57.1	0.797
2/3-Muscle	42.07	0.646
Bone Cancellous	22.4	0.235
Blood	57.29	1.72
Cartilage	43.64	0.65

implanted antennas for higher frequencies, we need to define the electromagnetic properties of the materials. Classical antenna theory mainly deals with antennas placed in a vacuum or in air, which is a non-conducting environment and has a permittivity of $\varepsilon_0 = 8.854 \cdot$ 10-12 F/m. With a higher permittivity and non-zero conductivity environment, theory must be revised from the usual simplifications used in antenna design. The permittivity ε and the conductivity σ of a medium are defined in their real and imaginary parts as (1) and (2). The complex permittivity defined from the effective permittivity ε and the conductivity σ is defined as (3).

$$\varepsilon = \varepsilon^{'} - j\varepsilon^{*} \tag{1}$$

$$\sigma = \sigma^{'} - j\sigma^{*} \tag{2}$$

$$\varepsilon_0 = \varepsilon_e - j\frac{\sigma_e}{\varepsilon_0 \omega} \tag{3}$$

The effective dielectric and conductive properties of human tissue have been characterized as described by (4) and (5). The loss due to conductivity in matter is often expressed as a dissipation factor or a loss tangent tanδ. They are defined as (6) where the imaginary parts of ε and σ are due to time lags in the electromagnetic response of the materials [17]. Specifically, ε" is due to the polarization response of the material and σ" is mainly due to time lag in the conduction response caused by large ions. The effective permittivity ε_e and conductivity σ_e of different human tissues are relevant for medical implants and are given in Table 1. All data is given for a frequency of 403.5 MHz and are from [18]. The frequency-dependent relative permittivity and conductivity [19] of skin (wet and dry), fat, blood, and muscle are shown in Figs. 3 and 4. A shift in resonant frequency was studied to determine the characteristic of blood glucose level in three conditions (hypoglycemia, hyperglycemia, and normoglycemia) [20]. The relative permittivity used for the 2/3-mucle tissue regarding to the blood glucose level on resonant frequency is shown in Fig. 5.

$$\varepsilon_e = \varepsilon' - \frac{\sigma"}{\omega} \tag{4}$$

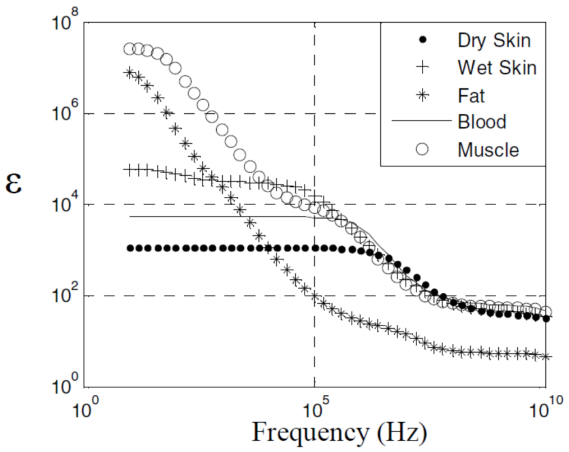

Fig.3: *Biological Tissue Model Relative Permittivity [18].*

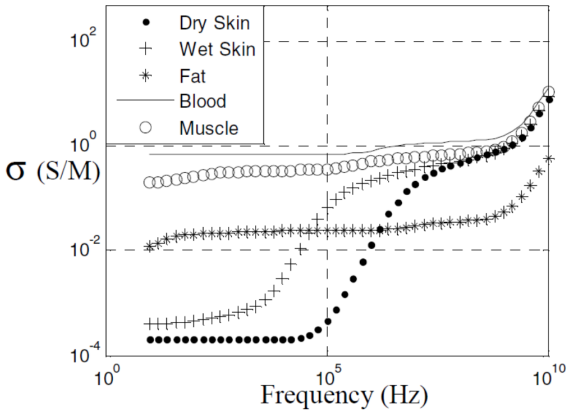

Fig.4: *Biological Tissue Model Relative Conductivity [18].*

$$\sigma_e = \sigma' + \omega\varepsilon" \tag{5}$$

$$tan\delta = \frac{\sigma_e}{\omega\varepsilon_e} \tag{6}$$

3. METHOD OF ANALYSIS, EVALUATION AND OPTIMIZATION

The Finite Different Time Domain (FDTD) method is used to simulate the microstrip antennas. From the previous work it has been observed that for the purposes of optimization, the FDTD simulation can be relatively imprecise while still yielding relative performance metrics that lead the optimization to a good design. Thus, completed convergence, ideal boundary conditions, and etc. are compromised for the sake of computational speed in this already computationally intensive process. The grid size is Δx = Δy = Δz = 1 mm and later is changed into 0.5 mm. The perfect matched layer (PML) absorbing boundaries are 160 cells away from the antenna model. The analysis with the general features is as follows.

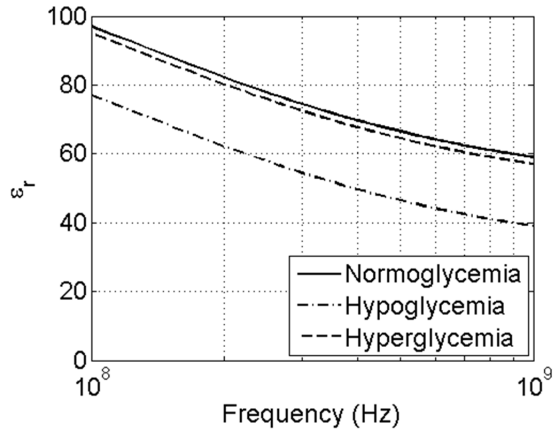

Fig.5: *Relative Permittivity Used in Antenna Simulation.*

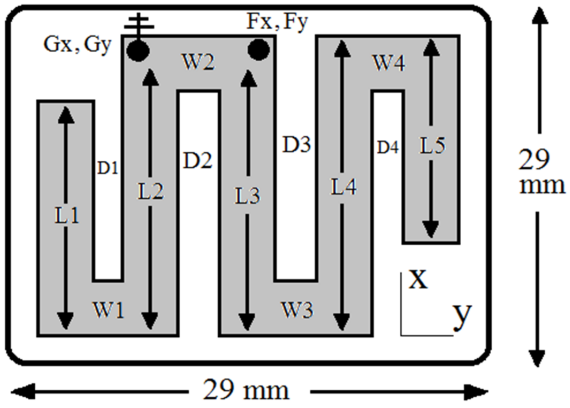

Fig.6: *Top View of the Antenna.*

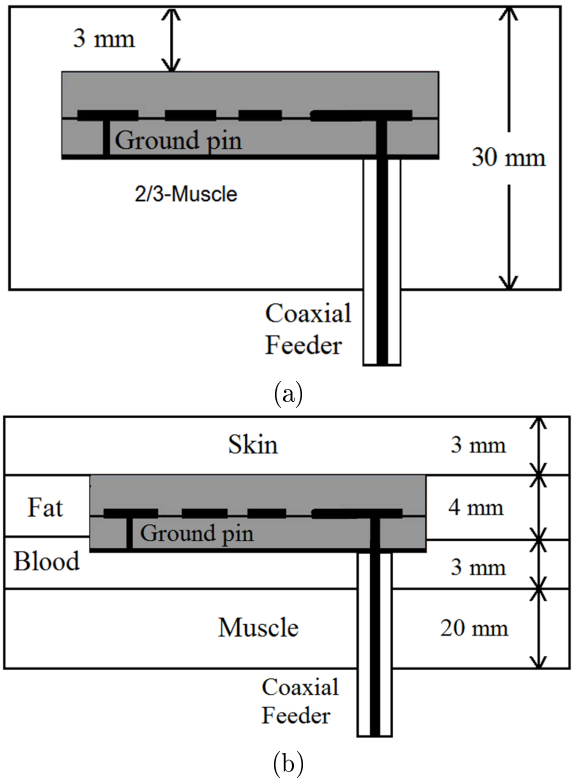

Fig.7: *Human Body Tissue Model (a) 2/3-Muscle and (b) a Simplified Four-Layer.*

A. Initial Serpentine PIFA Design

The initial antenna design is shown in Fig. 6. The radiation width is 3 mm and other parameter are as follow: L1 = 22, L2 = 22, L3 = 22, L4 = 22, L5 = 11, D1 = 4.5, D2 = 3, D3 = 4.5, D4 =3, W1 = W2 = W3 = W4 = 3, Fx = 0, Fy = -4, Gx = Gy = 0; the unit is in mm. The Rogers RO3210 (ε_r = 10.2, tanδ = 0.003) is used for the substrate and superstrate material. A shorting pin is used to assist in antenna miniaturization. The pin behaves like a ground plane and increases the electrical length of the serpentine. First the antenna is embedded in a 140 mm x 140 mm x 30 mm block of 2/3 muscle as shown in Fig. 7a. The 2/3 human muscle is commonly used to represent average body properties. The electric properties are 2/3 those of pure muscle (ε_r = 42.807 and σ = 0.6463 S/m for normoglycemia). For hypoglycemia and hyperglycemia, the electrical properties are ε_r = 38.12 with σ = 0.85 S/m and ε_r = 47.97 with σ = 0.59 S/m, respectively. The simplified model helps speed the simulation time. Finally a four-layer phantom similar to those in a human chest is used to simulate the performance of the antenna in the presence of four different tissue layers (skin, fat, blood, and muscle). Skin 3 mm thick was placed on top of a 4 mm fat layer, a 3 mm blood layer and a 20 mm muscle layer as shown in Fig. 7b. The antenna location was carefully selected in order to match the real implanted location. The antenna was placed between the skin and muscle tissues within the superstrate layer underneath the skin. These tissues and their processes are similar to [9]. The XFDTD provided by Remcom [21] has been used for all simulation processes.

Fig. 8 shows the simulated return loss of the initial design. Note that measured skin properties are used from [22-23] during simulations. The operating frequency between the antenna implanted in a 2/3-mucle model and in a simplified four-layer model are slightly different. Still, a 2/3 muscle can be used to predict the trend and it can speed the simulation process by 30-40 percent. In a simplified model, the antenna resonates at 388 MHz in hyperglycemia, 418 MHz in hypoglycemia and 402 MHz in normoglycemia level. The total frequency shifted from hyperglycemia to hypoglycemia in a 2/3-muscle and in a simplified model is 22 MHz and 30 MHz, respectively. Although close, the results do not match the desired frequency at 402-405 MHz, and the return loss is higher than 10 dB for hypoglycemia and hyperglycemia conditions. To tune and improve the antenna characteristics, a genetic algorithm optimization is applied.

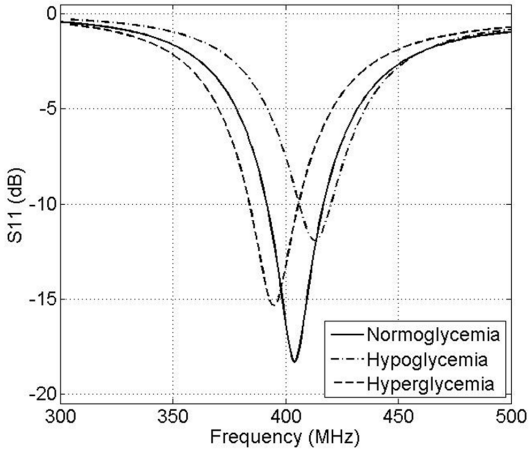

(a)

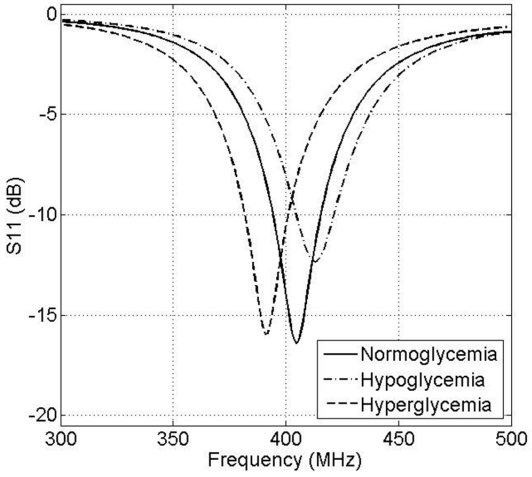

(b)

Fig.8: *Return Loss of the Antenna in (a) 2/3-Muscle and (b) a Simplified Four-Layer.*

B. Genetic Algorithm Optimization

The initial objective of this work is to design a microstrip antenna with a reflection coefficient lower than 15 dB in the 402-405 MHz MICS band for all glucose conditions. Although it was well achieved in the normoglycemia, the resonant frequency failed to perform in hypoglycemia and hyperglycemia. The reflection coefficient at the communication frequency should be as insensitive to glucose level as possible, so that varying dielectric properties does not de-tune the antenna performance. The optimization technique requires the cost function (magnitude of the reflection coefficient) to be evaluated for each test antenna, which is represented by its own GA chromosome. Each chromosome is composed of genes that describe a sequence of binary bits containing antenna design parameters to be optimized.

For the optimization procedure, the antenna geometry was organized as shown in Fig. 6, while maintaining the configurations and dielectric properties for a phantom model as described in the previous section. The dimensions of the substrate and superstrate were kept constant at L = 29 mm and W = 29 mm and the dimensions of the patch (length and width) were 25 mm and 25 mm, respectively. The other parameters, L1, L2, L3, D1, D2, D3, D4, W1, W2, W3, W4, Fx, Fy, Gx, and Gy were determined in the chromosome array. The feed and ground pins were allowed to move along the x-axis and y-axis, but with movement constrained by the antenna shape and were forced to attach to the radiated part. This method has been used in the past to design antennas implanted in the human body. The coordinates of the center of the feed and shorting pins were calculated and the parameters resulted in a 17-dimension solution space with possible values listed in Table II.

The goal of the optimization is improving antenna performance around the center frequency of MICS band (403.5 MHz). Therefore the fitness function of this problem is chosen to be as (7)

$$fitness = max(S_{11\ k1}, S_{11\ k2}, S_{11\ k3}) \qquad (7)$$

where ($S_{11\ k}$ refers to the return loss at a sample frequency point at 403.5 MHz, and the subscript 1, 2 and 3 indicates glucose levels at hypoglycemia, normoglycemia and hyperglycemia, respectively. With an objective function emphasizing communication, more weight was placed on the frequency difference to minimize the effect of glucose level. This objective function can be combined with other criteria based on radiation pattern and power requirements, but at this point, we focused only on the return loss optimization. The parameters of the evaluation, crossover and mutation were: population size = 48, discard rate = 0.4-0.6 and mutation rate = 8-15%. The optimized process was set for 250 iterations.

The optimized parameters are shown in Table 2 and the antenna model is shown in Fig. 9. The simulated return loss of the optimal design for all three glucose conditions are shown in Fig. 10. The E-field radiation patterns (at a distance of 1 meter) at the communication band 402 MHz for the antenna are shown in Fig. 11. The results in term of s-parameter, bandwidth and 1g-SAR are compared to those of the model in the presence of three different glucose levels as shown in Table 3.

C. Effect of Nonuniform Model

From the relative permittivity and the return loss plots in Figs. 5 and 8, the glucose levels changing from hypoglycemia to hyperglycemia mainly affected the relative permittivity and conductivity of a blood layer. A novel approach to determine a tight glucose sensing for patients with diabetes could be based on measuring the changes in antenna performances of glucose-sensitive surrounding tissues. In order to achieve the goal of a long-term implantable glucose sensor, the effect of nonuniform electrical properties

Table 2: *Serpentine Optimization Parameters.*

Parameters	Range (mm)	Optimized (mm)
L1	[20, 25]	24
L2	[22, 25]	22.5
L3	[22, 25]	22.5
L4	[20, 25]	21
L5	[8, 25]	12
D1	[1.5, 4.5]	2.5
D2	[1.5, 4.5]	3
D3	[1.5, 4.5]	1.5
D4	[1.5, 4.5]	2
W1	[1.5, 4.5]	3
W2	[1.5, 4.5]	2.5
W3	[1.5, 4.5]	4
W4	[1.5, 4.5]	4.5
Fx	[-1, 22]	8
Fy	[-5, 16]	0.5
Gx	[-1, 22]	0.5
Gy	[-5, 9]	1

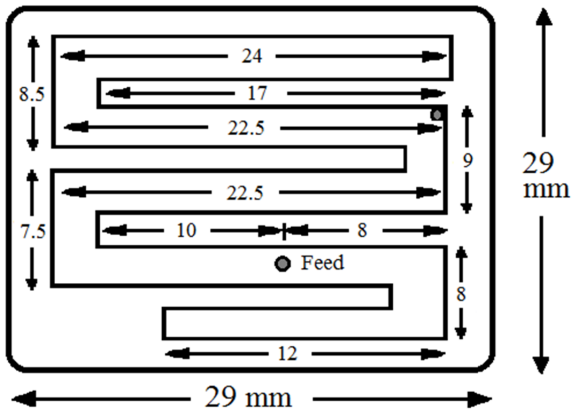

Fig.9: *The optimized Design (unit in mm.)*

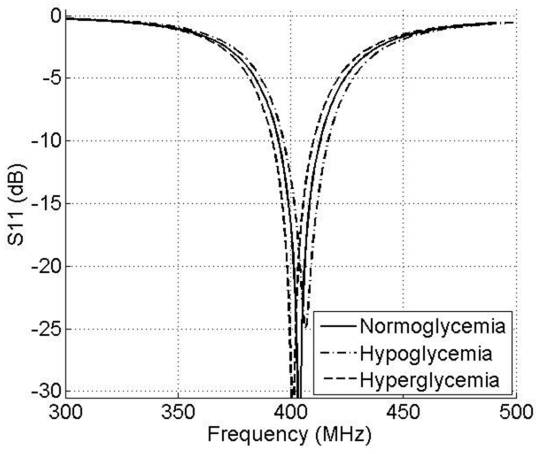

Fig.10: *Simulated Return Loss of the Antenna in Fig. 9.*

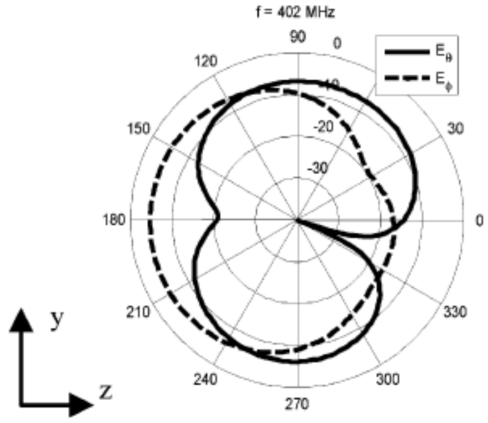

Fig.11: *Far-Field Patterns for 402 MHz.*

Table 3: *Comparisons of the antenna performance in three different glucose levels*

Parameter	Hypo glycemia	Normo glycemia	Hyper glycemia
S_{11} (dB)	-20.4	-29.3	-21.5
1g-SAR (mW/kg)	48.9	49.3	49.8
SAR max (mW)	137.1	126.5	159.1
G_{max} (dB)	-29.5	-29	-29.2
Efficiency (%)	6.2	6.7	6.1

of all four-layer geometry is also of interest. The dielectric properties of skin, fat, blood, and muscle are reevaluated in the case that they were consumed by glucose.

In order to test this possibility, the percentages of glucose level that might be allowed to permeate the four-layer geometry were controlled by soaking addition layer. In this case, it was assumed that the glucose level have permeated into the fat and skin layers, and thus affected the dielectric properties with some percentages from the hypoglycemia to hyperglycemia. For hypoglycemia the dielectric properties of layer with 10% body fluid are assumed to be ε_r = 3.8 and σ = 0.08 S/m, and with 20% body fluid ε_r = 7.6 and σ = 0.16 S/m. And for hyperglycemia the dielectric properties of layer are ε_r = 4.7 with σ = 0.059 S/m and ε_r = 9.4 with σ = 0.118 S/m for 10% and 20% respectively. The antenna model from Fig. 9 is used to demonstrate these assumption. The results of the non-uniform electrical properties for the four-layer geometry are shown in Table 4. The differences in the resonant frequency, 1g-SAR level and the corresponding relative gain at delivered power of 1 mW are observed. It is shown that the antenna failed to maintain its performance under the nonuni-

Table 4: *The 1g SAR, maximum gain comparison in the body model at delivered power of 1 mW from the antenna.*

Type	Resonant Frequency (MHz)	1g-SAR (mW/Kg)	G_{max} (dB)
20% Hypoglycemia	386	49.6	-31.8
10% Hypoglycemia	391	49.7	-31.2
Hypoglycemia	410	48.9	-29.5
Normoglycemia	403	49.3	-29
Hypoglycemia	400	49.8	-29.2
10% Hyperglycemia	387	49.9	-30.6
20% Hyperglycemia	381	50.1	-31.1

form condition. It is worth noticed that though SAR level has less impacted, the maximum gain is almost 3 dB different.

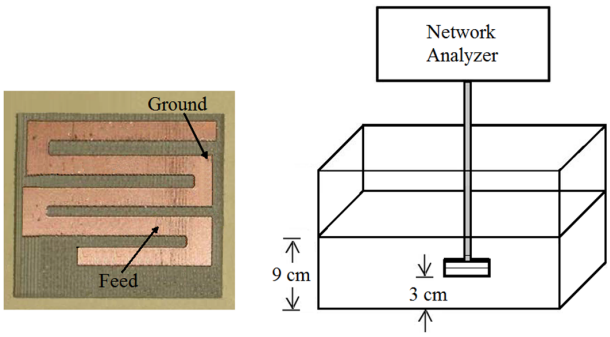

Fig.12: *Return-loss measurement setup for resonant characteristics of the designed antenna.*

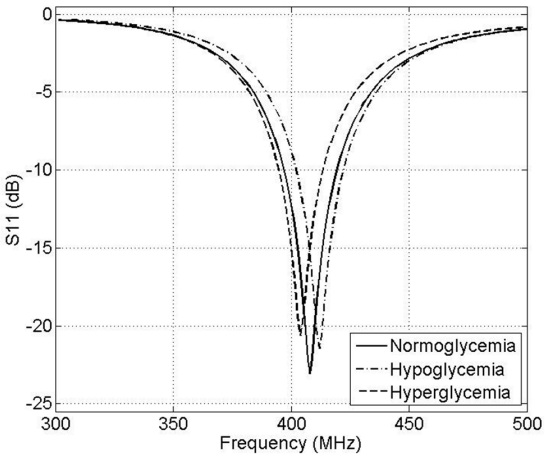

Fig.13: *Measured Return Loss of the Fabricated Antenna.*

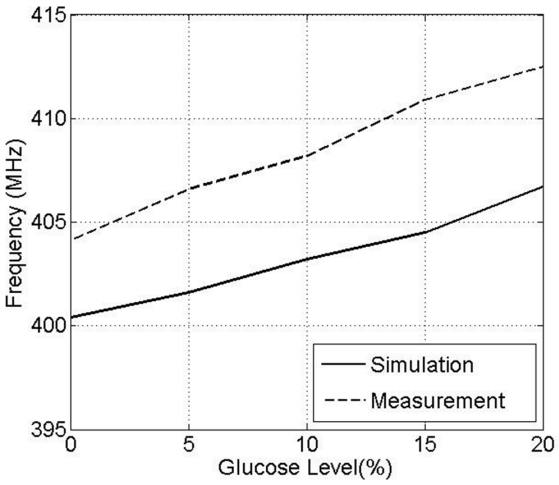

Fig.14: *Location of the First Null for Various Glucose Levels.*

4. PROTOTYPE AND MEASUREMENT RESULTS

To verify the simulation results, a prototype of the antenna was built from Rogers RO3210 (ε_r=10.2, tanδ=0.003) substrate, and the antenna was buried 30 mm deep in a block of tissue stimulant material. This material consisted of TX-151 powder, sugar, salt, and deionized water. Measured values of hypoglycemia and hyperglycemia have dielectric permittivity of 39.78 and 49.23 and conductivity 0.93 and 0.54 S/m, respectively. The antenna prototype and the return losses of the antenna are shown in Figs. 12 and 13, respectively. Agreement between the measured and simulated values is reasonable within the expected range of modeling, considering the coarseness of the simulations, and the prototype antenna meets the expectations of the cost function. Good agreement is expected and achieved for the MICS band. The 10-dB bandwidths of the simulation and the measurement in the MICS region are 25.3% and 20.4%, respectively. The simulation and measurement comparison of the null in different glucose levels is shown in Fig. 14. The relatively flat performance of the first null is desired and is achieved up to about 20% glucose levels for the simulation and about 15% glucose levels for the prototype measurement.

5. CONCLUSIONS

In this study, we designed and tested an implantable antenna operating at 402-405 MHz MICS band intended for biomedical devices. The implanted antenna can work effectively regardless of different glucose levels. Thus, this antenna can be applied for continuous glucose-monitoring applications. Using the genetic algorithm (GA) and the finite difference time domain (FDTD) method, the antenna is

designed to have minimal detuning due to changes in blood glucose levels. In order to test the performance of the antenna, we developed three simulant tissues to mimic the electrical properties of the real human body in hypoglycemia, normoglycemia and hyperglycemia. The fabricated antenna was embedded in these gels and tested using an HP8510C network analyzer. The results were compared with the simulations, and an excellent agreement was observed. The measured antenna had dimensions of 29 mm $\times$ 29 mm $\times$ 3 mm. The obstacle during measurement was to make stimulant gels that have the dielectric properties similar to those of the human body for three glucose levels. While we have successfully accomplished this task for designing an implanted antenna able to communicate in the MICS band regardless of different glucose levels, there is still needed for an implanted antenna as a sensing device. Moreover with the nonuniform body layer, the resonant frequency is moved out of the MICS band and lost its maximum gain power. Therefore we are currently working to perfect the antenna that is less sensitive to nonuniform body and a dual band implantable antenna for continuous monitoring applications. Finally, based on the limitations for biomedical telemetry devices, more sensitive receivers which are able to function within a wider range of frequencies are necessary for reliable communication links between the designed antennas and exterior devices.

6. ACKNOWLEDGEMENT

This research material was based upon work supported by the Thailand Research Fund (TRF) under Grant No. MRG5280193.

References

[1] The American Diabetes Association, 2013, *Diabetes reports 2013* [Online]. available: http://www.diabetes.org

[2] Center for Disease Control and Prevention, 2013, *MMWR* [Online].available: http://www.cdc.gov

[3] P. Hossain, B. Kawar, M. El Nahas, "Obesity and diabetes in the developing world-a growing challenge," New England J. Medicine, vol. 356, no. 3, pp. 213-215, Jan. 2007.

[4] World Diabetes Foundation, 2013, *Diabetes detection* [Online]. available: http://www.worlddiabetesfoundation.org

[5] National Diabetes Information Clearinghouse, 2013, *National diabetes statistics* [Online]. available: http://diabetes.niddk.nih.gov

[6] International Diabetes Federation, 2013, *Diabetes aware* [Online]. available: http://www.Idf.org

[7] L. Xu, and M. Meng, "Effect of dielectric parameters of human body on radiation characteristic of ingestible wireless device at operating frequency of 430 MHz," *IEEE Trans. Biomed. Eng.*, vol. 56, no. 8, pp. 2083-2094, Aug. 2009.

[8] American National Standards Institute (ANSI), 2013, *SAR regulation* [Online]. available: http://www.ansi.org

[9] P. Soontornpipit, C.M. Furse, and Y. C. Chung, "Design of implantable antennas for communication with medical implants", *IEEE Trans. MTT*, vol. 52, issue 8, pp. 1944-1951, Aug. 2004.

[10] P. Soontornpipit, C. M. Furse, and Y. C. Chung, "Miniaturized biocompatible microstrip antenna using a genetic algorithm", *IEEE Trans. Antennas Propag.*, vol. 53, no. 6, pp. 1939-1945, Jun. 2005.

[11] P. Soontornpipit, "Radiation characteristics and SAR effects of wireless implant medical devices in human Body", *Asian J. Tropical Medicine Public Health*, vol. 5, pp. 231-238. Aug. 2012.

[12] P. Soontornpipit, "Study of 403.5 MHz path loss models for indoor wireless communications with implanted medical devices on the human body," *ECTI Trans. Elect. Eng., Electron., Commun.*, vol. 10, no. 2, pp. 165-170, Aug. 2012.

[13] S. Kwak, K. Chang, and Y. J. Yoon, "Ultra-wide band spiral shaped small antenna for the biomedical telemetry," *Proc. Asia-Pacific Microw. Conf.*, vol. 1, pp. 241-244, Dec. 2005.

[14] A. Kiourti, and K. S. Nikita, "A review of implantable patch antennas for biomedical telemetry: challenges and solutions," *IEEE Antennas Propag. Mag.*, vol. 54, no. 3, pp. 210-228, Jun. 2012.

[15] Medical implant communications service (MICS) federal register, 2013, *FR regulatory*, [Online]. available: https://www.federalregister.gov/articles/1999/12/15/99-32454.

[16] D. Flamm, "Biocompatible materials for microstrip pacemaker antenna", Senior Project, Electrical Engineering, Utah State University, 2002.

[17] R. W. P. King, and S. G. S., "Antennas in matter," *The MIT Press*, 1981.

[18] C. Gabriel, "Compilation of the dielectric properties of body tissues at RF and microwave frequencies," Brooks Air Force, technical report AL/OE-TR-1996-0037, 1996.

[19] S. Gabriel, R.W. Lau, and C. Gabriel, "The dielectric properties of biological tissues: II. measurements in the frequency range 10 Hz to 20 GHz," *Phys. Med. Biol.*, vol. 41, no. 11, Nov. 1996.

[20] B. Freer, and J. Venkatalaman, "Feasibility study for non-invasive blood glucose monitoring," *Proc. Antennas Propag. Soc. Int. Symp.*, pp.1-4, 2010.

[21] Remcom Inc, 2013, *Finite different time domain (FDTD) tutorial*, [Online]. available: http://remcom.com

[22] M. Yvanoff, and J. Venkataraman, "A feasibility study of tissue characterization using LC sensors" *IEEE Trans. Antennas Propag.*, vol. 57, no. 4, Apr. 2009.

[23] C. Gabriel, S. Gabriel, and E. Corthout, "The dielectric properties of biological tissues: I. literature survey," *Phys. Med. Biol.*, vol. 41, pp. 2231-2249, Apr. 1996.

Pichitpong Soontornpipit received the B.S. degree from the Mahanakorn University of Technology, Bangkok, Thailand in 1997, the M.S. degree from Utah State University in 2001, and the Ph.D. degree from the University of Utah, USA, in 2005. He was with the Center for Self Organizing Intelligent Systems and the Center of Excellence for Smart Sensors at the University of Utah. He was an Antenna Design Engineer with Laird Technology, San Diego, CA. He currently is lecturer with the Department of Health Informatics, Public Health of Mahidol University. His research interests include computational electromagnetics, optimized antennas, conformal and fractal antennas, RFID, UWB, smart wireless sensors, and implanted medical and health care systems.